Original Research Article

Analytical and Numerical studies of transient heat transfer in soil for geothermal systems

ABSTRACT

The study of geothermal systems requires a good knowledge of heat transfers in the depth of the soil. The aim of this work is to study the distribution of temperature in the ground under the climatic conditions of Togo. The analytical and numerical solutions of unidirectional heat transfer equation assuming the soil as a semi-infinite medium are found. The analytical solution is validated with the work of Benhammou. The comparison of the results of Benhammou and the present works shows a good qualitative agreement. The results show that depending on the meteorological conditions, the outdoor air undergoes strong variations in temperature and humidity. On the other hand, the ground, a few meters below its surface, has a slight variation in temperature due to its high thermal inertia. The nature of the soil, the latent exchanges of water evaporation and the characteristics of the vegetation cover also affect strongly on the soil temperature. These findings are very important for the installation of air/soil heat exchangers (for cooling/heating buildings) or bioreactor installations for biogas production.

Keywords: Renewable energy, Geothermal energy, Penetration depth, Soil temperature.

1. INTRODUCTION

In civil engineering structures such as buildings, roads and airport runways, geothermal systems, bioreactors,... soil temperature plays a main role in their implementation. In recent years numerous works have been carried out on the determination of soil temperature by analytical methods, numerical methods and experimental studies [1-8].

Mahdi MH et al. [9] studied analytically soil temperature with respect to its salinity. The study shows a direct relationship between the soil salinity and the temperature rising. To estimate soil temperature more accurately, Guojie H et al. [10] proposed a solution method of the heat conduction equation of soil temperature by employing both the improved heat conduction model and the classical heat conduction model to fit soil temperature. The results showed that the daily soil temperature amplitude can be better described by the sinusoidal function in the improved model, which then yielded more accurate soil temperature simulating effect. Benhammou et al [11] studied the influence of soil nature on soil depth temperature, as well as on the phase shift and penetration depth of the temperature signal. This study was carried out under the meteorological conditions of the city of Adrar in Algeria. The results obtained indicate that the annual penetration depth as well as the phase shift are greatly influenced by the nature of the soil, while the average temperature of the soil surface is insensitive to it. Sodha et al. [12] obtained the variance of soil temperature using the Fourrier coefficient approach and predicted that the variance decreases rapidly with depth and the temperature becomes constant from 0.4 m depth. A practical approach to predict soil temperature variations for soil heat exchangers applications is adopted by Onder

Ozgener et al. [13]. Transient heat flow principles were used with assumptions of one dimensional heat flow, homogeneous soil, and constant thermal diffusivity. Measured and predicted soil temperatures at different depths were compared with experimental field results to validate the accuracy of the current model. Accepting that the model results are approximate and depend on the theoretical approach and assumptions employed, the estimated errors are still in an acceptable range for calculation of heating and cooling design parameters substantially reducing the need for detailed site surveys. A literature review was carried out by Bowen et al. [14] on passive and hybrid cooling of buildings. It appears that earth cooling is based on the temperature difference between soil and the atmospheric environment. During the summer, the soil temperature at certain depth is considerably lower than the ambient temperature and therefore offers an important source for the dissipation of the building excess. Zhan M et al. [15] evaluated and analyzed the soil temperature Data over Poyang Lake Basin in China. The results show that, the climatic trend of soil temperature generally increased from south to north, which was opposite to the distribution of soil temperature. These findings provide a basis for understanding and assessing the variation of soil temperature in the Poyang Lake Basin. Numerical study for soil temperature is carried out by Singh RK et al. [16]. Finite difference method has been used to discretize computational domain and the heat transfer equation. The results show that the diurnal temperature variation is found up to 0.4 m depth of soil whereas annual temperature variation is up to a depth of 4 m.

The main objective of this work is to propose heat transfer models for determining the temperature in the ground and then integrating it into a geothermal system such as the air-soil exchanger or bioreactors facilities.

2. METHODOLOGY

2.1 Heat transfer modelling in soil

2.1.1 Heat transfer model in a semi-infinite soil without vegetation cover

2.1.1.1 Physical model and simplifying assumptions

The physical model of the problem is depicted in Image 1. The space is divided into two parts: the solid mass of the soil and the atmosphere above the surface of the ground. The surface of the ground exchanges heat by convection with the atmosphere and by conduction through the solid mass influenced by the solar radiation of the site.

Image. 1. Semi-infinite model of the ground

To simplify the heat transfer equation of the ground, the following assumptions are considered:

- the temperature of the ground is less varying along the surface. However, it changes on depth. Thus, the temperature of the ground is unidirectional along the depth.
- the soil is assumed to be a semi-infinite medium;
-there is no internal heat sources in the solid mass of soil;
- for the analytical model, the soil is assumed to be without vegetation cover; convection on the soil is neglected; absorbed radiation is not re-emitted; the soil has homogeneous and constant thermal properties; the thermal effusivity of the uncovered surface of the ground is very high.
- for the numerical model, the ground is covered of vegetation characterized by the LAI (Leaf Area Index). It is a dimensionless quantity that characterizes the vegetation cover defined as the one-sided green leaf area per unit ground area (LAI = leaf area/ground area, m^2 /m^2) in broadleaf canopies. Soil conductivity is variable. The temperature of surface of the ground is affected by coupled heat transfer radiation and convection with ambient.

The physical model is associated with an unidirectional cartesian coordinate system whose origin is located on the surface of the ground. The axis is vertical and oriented downwards.

2.1.1.2 Heat conservation equation in soil

Conduction is a transmission of heat in matter by molecular or atom vibration. The thermal vibrations of crystals are due to the excited phonons.
Based on Fourier law, the general heat transfer equation for three-dimensional conduction can be expressed as follow:

$$\rho_{soil} C_{psoil} \frac{\partial T_{soil}}{\partial t} = \lambda_{soil} \left(\frac{\partial^2 T_{soil}}{\partial x^2} + \frac{\partial^2 T_{soil}}{\partial y^2} + \frac{\partial^2 T_{soil}}{\partial z^2} \right) + \dot{Q}_{soil} \quad (1)$$

where T_{soil} is the temperature of the soil (K), a function of the coordinates (x,y,z) of the considered point of the soil and the time t (s). The parameters, ρ_{soil}, C_{psoil} and λ_{soil} define the physical properties of the soil and represent respectively, density (k_g / m^3), specific heat capacity at constant pressure ($J.kg^{-1}.K^{-1}$) and thermal conductivity ($W.m^{-1}.K^{-1}$).
For a one-dimensional transfer along the z-axis, T_{soil} is independent of the x,y space variables (*m*) and can be written as :

$$\frac{\partial T_{soil}}{\partial x} = \frac{\partial T_{soil}}{\partial y} = 0 \quad (2)$$

and as a result:

$$\frac{\partial^2 T_{soil}}{\partial x^2} = \frac{\partial^2 T_{soil}}{\partial y^2} = 0 \quad (3)$$

Equation (1) becomes:

$$\rho_{soil} C_{psoil} \frac{\partial T_{soil}}{\partial t} = \lambda_{soil} \frac{\partial^2 T_{soil}}{\partial z^2} + \dot{Q}_{soil} \quad (4)$$

In the absence of internal heat sources in the soil,

$$\dot{Q}_{soil} = 0 \quad (5)$$

The simplified equation is then written:

$$\rho_{soil} C_{psoil} \frac{\partial T_{soil}}{\partial t} = \lambda_{soil} \frac{\partial^2 T_{soil}}{\partial z^2} \quad (6)$$

or: $$\frac{\partial T_{soil}}{\partial t} = \left(\frac{\lambda_{soil}}{\rho_{soil} C_{psoil}} \right) \frac{\partial^2 T_{soil}}{\partial z^2} \quad (7)$$

By setting :

$$\alpha_{soil} = \frac{\lambda_{soil}}{\rho_{soil} C_{psoil}} \quad (8)$$

Equation (7) can be written as :

$$\frac{\partial T_{soil}}{\partial t} = \alpha_{soil} \frac{\partial^2 T_{soil}}{\partial z^2} \quad (9)$$

where α_{soil} is the thermal diffusivity of the soil (m^2/s).

2.1.1.3 Variation of the ambient temperature

The variation of the ambient temperature $T_{amb}(t)$ (K) can be approximated by a sinusoidal function of period T (s) based on the average temperature T_0 (K), amplitude A_T (K) phase φ (rad) corresponding to the period considered (daily, monthly or yearly).

$$T_{amb}(t) = T_0 + A_T Cos\,(\omega t - \varphi) \quad (10)$$

where T_0, A_T and φ, are the constants.

Let us determine the constants T_0, A_T and φ

It is considered T_{min} and T_{max} respectively, the minimum and maximum temperatures (*K*) over the time interval of length equal to the period T considered.

The ambient temperature is minimum if the value of $Cos\,(\omega t - \varphi)$ is minimum, i.e. :

$$Cos\,(\omega t - \varphi) = -1. \quad (11)$$

It is obtained:

$$T_{min} = T_0 - A_T \quad (12)$$

The outdoor temperature is maximum if the value of $Cos\,(\omega t - \varphi)$ is maximum, i.e.

$$Cos\,(\omega t - \varphi) = -1 \quad (13)$$

and:

$$T_{max} = T_0 + A_T \quad (14)$$

Combining the relations (12) and (14) we get :

$$T_0 = \frac{T_{max}+T_{min}}{2} \quad (15)$$

$$A_T = \frac{T_{max}-T_{min}}{2} \quad (16)$$

Let us denote by t_0, the instant corresponding to the highest temperature over this time interval (s).

$$Cos\,(\omega t_0 - \varphi) = -1 \quad (17)$$

$$\omega t_0 - \varphi \equiv 0[2\pi] \quad (18)$$

$$\varphi \equiv \omega t_0[2\pi] \quad (19)$$

The relation (10) becomes:

$$T_{amb}(t) = T_0 + A_T Cos\,[\omega(t - t_0)] \quad (20)$$

2.1.1.4 Boundary conditions

-At the ground surface: Z=0

For simplification purposes, as the ground surface is in direct contact with the atmosphere, it is assumed that the ground surface temperature is that of the atmosphere (outside air). We can therefore write :

$$T_{soil}(0,t) = T_{amb}(t) \quad (21)$$

where $T_{amb}(t)$ is the ambient temperature.

-At an infinite depth (Z=∞)

Since the soil is considered a semi-infinite medium, the dimensions of the soil are large enough that edges other than the surface (z=0) have no practical impact on the system in the time interval considered. Thus the soil temperature at infinite depth is equal to the average value taken between the minimum and maximum temperature (T_0) over the time interval corresponding to period T of the sinusoidal exciting temperature of the ambient air.

Thus:

$$T_{soil}(\infty,t) = T_0 \quad (22)$$

2.1.1.5 Analytical solution

The heat equation and boundary conditions are given by:

$$\frac{\partial T_{soil}}{\partial t} = \alpha_{soil} \frac{\partial^2 T_{soil}}{\partial z^2} \quad (23)$$

with:

$$T_{soil}(0,t) = T_{amb}(t) \quad (24)$$

$T_{soil}(\infty, t) = T_0$ (25)

Change of variable :

Let us consider

$\theta = T - T_0$ (26)

$T = \theta + T_0$ (27)

By replacing (27) in equation (23), the heat equation becomes :

$\frac{\partial \theta}{\partial t} = \alpha_{soil} \frac{\partial^2 \theta}{\partial z^2}$ (28)

The boundary conditions (24) and (25) become:

$\theta(0, t) = A_T cos[\omega(t - t_0)]$ (29)

$\theta(\infty, t) = 0$ (30)

when x tends to infinity, the temperature is finite, so the solution of equation (28) takes the form:

$\theta(z, t) = f(z)g(t)$ (31)

$\frac{\partial^2 \theta}{\partial x^2} = f"(z)g(t)$ (32)

$\frac{\partial \theta}{\partial t} = f(z)g'(t)$ (33)

Substituting the relations (32) and (33) into the heat equation (28), we obtain:

$f(z)g'(t) = \alpha_{soil} f"(z)g(t)$ (34)

or:

$\alpha_{soil} \frac{f"(z)}{f(z)} = \frac{g'(t)}{g(t)}$ (35)

then:

$\frac{g'(t)}{g(t)} = \beta$ (36)

$\alpha_{soil} \frac{f"(z)}{f(z)} = \beta$ (37)

where β is a constant.

Let us solve equation (36):

Equation (36) can be written as :

$\frac{dg(t)}{dt} - \beta g(t) = 0.$ (38)

Since the excitation is periodic in nature, we must look for a solution with the same frequency as the excitation by posing :

$\beta = i\omega$ with $i^2 = -1$.

The problem can be solved in the complex plane and only the real part of the solution obtained will be retained.

$\frac{dg(t)}{dt} - i\omega g(t) = 0$ (40)

$\int \frac{dg(t)}{g(t)} = \int \beta i\omega dt$ (41)

$lng(t) = i\omega t + K;\ g(t) = Aexp(i\omega t)$ (42)

where K and A are constants.

Let us solve equation (37):

Equation (37) is written as:

$\alpha_{sol} f"(z) - i\omega f(z) = 0$ (43)

The characteristic equation of the differential equation in function of the characteristic variable r, is given by:

$\alpha_{soil} r^2 - i\omega = 0$ (44)

$r^2 = \frac{i\omega}{\alpha_{soil}}$ (45)

$r^2 = \frac{\omega}{\alpha_{soil}} exp\left(\frac{\pi}{2}\right)$ (46)

Let's pose:

$r = r_0 e^{i\varphi}$ (47)

$r^2 = r_0^2 e^{i2\varphi}$ (48)

The relations (46) and (48) give:

$r_0^2 = \frac{\omega}{\alpha_{soil}}$ and $2\varphi \equiv \frac{\pi}{2}[2\pi]$ (49)

$r_0 = \sqrt{\frac{\omega}{\alpha_{soil}}}$ and $\varphi \in \left\{\frac{-3\pi}{4}, \frac{\pi}{4}\right\}$ (50)

Hence

$r_1 = -(1+i)\sqrt{\frac{\omega}{2\alpha_{soil}}}$ ou $r_2 = -(1+i)\sqrt{\frac{\omega}{2\alpha_{soil}}}$ (51)

where:

$f(z) = A'exp(r_1 x) + Bexp(r_2 x)$ (52)

or:

$$f(z) = A'exp\left((1+i)x\sqrt{\frac{\omega}{2\alpha_{soil}}}\right) + Bexp\left(-(1+i)z\sqrt{\frac{\omega}{2\alpha_{soil}}}\right) \quad (53)$$

As $f(z)$ must tend to a finite limit when $z \to \infty$, then $A' = 0$

We obtain :

$$f(z) = Bexp\left(-(1+i)z\sqrt{\frac{\omega}{2\alpha_{soil}}}\right) \quad (54)$$

The solution (31) of the heat equation is written:

$$\theta(z,t) = f(z)g(t) = AB.exp(i\omega t).exp\left(-(1+i)z\sqrt{\frac{\omega}{2\alpha_{soil}}}\right) \quad (55)$$

$$\theta(z,t) = C.exp(i\omega t).exp\left(-(1+i)z\sqrt{\frac{\omega}{2\alpha_{soil}}}\right) \quad (56)$$

Let 's pose:

$C = C_0 exp(i\emptyset)$ (57)

$$\theta(z,t) = C_0 exp(i\emptyset).exp(i\omega t).exp\left(-(1+i)z\sqrt{\frac{\omega}{2\alpha_{soil}}}\right) \quad (58)$$

$$\theta(z,t) = C_0 exp\left(-z\sqrt{\frac{\omega}{2\alpha_{soil}}} + i\left(\omega t + \emptyset - z\sqrt{\frac{\omega}{2\alpha_{soil}}}\right)\right) \quad (59)$$

The boundary condition (29) must verify the equation (59).

Therefore, we can write:

$\theta(0,t) = A_T cos\left[\omega\left(t - t_{0,}\right)\right] = R_e\left[C_0 exp\left(i(\omega t + \emptyset)\right)\right]$ (60)

$A_T cos\left[\omega\left(t - t_{0,}\right)\right] = R_e[C_0 cos(\omega t + \emptyset) + iC_0 sin(\omega t + \emptyset)]$ (61)

$A_T cos\left[\omega\left(t - t_{0,}\right)\right] = C_0 cos(\omega t + \emptyset)$ (62)

$A_T = C_0$ (63)

$\omega\left(t - t_{0,}\right) = \omega t + \emptyset$ and $\emptyset = -\omega t_0$ (64)

The relation (59) becomes :

$$\theta(z,t) = A_T exp\left(-z\sqrt{\frac{\omega}{2\alpha_{soil}}} + i\left(\omega(t - t_0) - z\sqrt{\frac{\omega}{2\alpha_{soil}}}\right)\right) \quad (65)$$

$$\theta(z,t) = A_T exp\left(-z\sqrt{\frac{\omega}{2\alpha_{soil}}}\right).exp\left(i\left(\omega(t - t_0) - z\sqrt{\frac{\omega}{2\alpha_{soil}}}\right)\right) \quad (66)$$

$$\theta(z,t) = A_T exp\left(-z\sqrt{\frac{\omega}{2\alpha_{soil}}}\right).\left[cos\left(\omega(t - t_0) - z\sqrt{\frac{\omega}{2\alpha_{soil}}}\right) + isin\left(\omega(t - t_0) - z\sqrt{\frac{\omega}{2\alpha_{soil}}}\right)\right] \quad (67)$$

The final solution of the heat equation is the real part of (67)

$$\theta(z,t) = A_T exp\left(-z\sqrt{\frac{\omega}{2\alpha_{soil}}}\right).cos\left(\omega(t - t_0) - z\sqrt{\frac{\omega}{2\alpha_{soil}}}\right) \quad (68)$$

with: $\omega = \frac{2\pi}{T}$; $\alpha_{soil} = \frac{\lambda}{\rho_{soil} C_{P,soil}}$; $d = \sqrt{\frac{2\,\alpha_{soil}}{\omega}}$; T_0 is the average temperature at the ground surface ; A_T amplitude of the oscillations of the temperature of the ground surface;

T period.
The amplitude of this thermal wave is expressed as:

$$A(z) = A_T.exp\left(-z\sqrt{\frac{\omega}{2\,\alpha_{soil}}}\right) \text{ where, } \frac{A(z)}{A(0)} = exp\left(-z\sqrt{\frac{\omega}{2\,\alpha_{soil}}}\right) = \epsilon_0 \quad (69)$$

with : ϵ_0, the attenuation accuracy of the thermal wave.
The attenuation depth is given by:

$$z_p = \frac{|ln(\epsilon_0)|}{\sqrt{\frac{\omega}{2\,\alpha_{soil}}}} \quad (70)$$

Now according to (26),

$$\theta(x,t) = T(x,t) - T_0 \quad (71)$$

therefore:

$$T(x,t) = T_0 + \theta(x,t) \quad (72)$$

$$T(x,t) = T_0 + A_T exp\left(-x\sqrt{\frac{\omega}{2\alpha_{soil}}}\right).cos\left(\omega(t-t_0) - x\sqrt{\frac{\omega}{2\alpha_{soil}}}\right) \quad (73)$$

2.1.2 Heat transfer model in a semi-infinite soil with a canopy

2.1.2.1 Physical model and simplifying assumptions

The physical and assumptions are described in section *2.1.1.1*. Therefore, here, the soil is assumed to a unidirectional layer of finite thickness e and the interface at z = e corresponds to the depth at which the conduction flux is zero.

2.1.2.2 Heat conservation equation in the soil

Taking into account the simplifying assumptions made above, the heat transfer equation is written as in (9):

$$\rho_{soil} C_{p,soil} \frac{\partial T_{soil}}{\partial t} = \frac{\partial}{\partial z}\left(\lambda_{soil} \frac{\partial T_{soil}}{\partial z}\right) \quad (74)$$

2.1.2.3 Boundary and initial conditions

- Boundary conditions

$$\lambda^e \frac{\partial T}{\partial z}\Big|_{z=e} = 0 \quad (75)$$

$$\alpha_s \phi(0) = -\lambda^e \frac{\partial T}{\partial z}\Big|_{z=0} + h_v(T - Tamb) + \varepsilon_s \Delta I_R + [C * f * h_v[(A.T + B) - HR(A.T_{amb} + B)] \quad (76)$$

where:

$$\varepsilon_s \Delta I_R = h_r\left(T - T_{sky}\right) \quad (77)$$

$$h_r = \varepsilon_s \sigma\left(T^2 + T_{sky}^2\right)\left(T + T_{sky}\right) \quad (78)$$

$$T_{sky} = 0.0552.T_{amb}^{1.5} \quad (79)$$

$$h_v = 0.5 + 1.5\sqrt{v_{wind}} \quad (80)$$

$\sigma = 5.670374419.10^{-8} W.m^{-2}.K^{-4}$ is Stephan constant.
h_r, h_v are heat transfer coefficient by radiation and convection ($W.m^{-2}.K$); T_{sky}, sky temperature (K). v_{wind}, wind speed ($m.s^{-1}$); ε_s, soil surface emissivity (dimensionless) ranges between 0 and 1; α_s, soil absorptivity (dimensionless) ranges also between 0 and 1.
The values of the empirical constants A, B and C are respectively:
$A = 103 Pa/k$; $= 609 Pa$; $C = 0.0168 K/Pa$ [11].
The values of the parameter f are given according to the soil type (Table 1)
- Initial conditions

$$T = T_0 \quad (81)$$

Table 1 Variation of the parameter f as a function of soil type [11].

Nature of the soil	f
Arid	0.1 – 0.2
Dry	0.4 – 0.5
wet	0.6 – 0.8
saturated	1.0

- If evaporation is neglected then f=0.
- if the soil is not covered by plants, then:

LAI=0 and $\phi(z' = 0) = \phi(0)$ (82)

- The canopy can intensely modify the heat transfers in the soil because the density that is received by the soil covered by plants is naturally attenuated through the vegetation cover layer. For a vegetation canopy, a leaf area density f(z') is defined as the ratio of the exchange area of the leaves to a unit volume (air and vegetation). Each level of vegetation is represented by f(z'). The cumulative leaf area F(z') is also defined from the desired canopy top:

$F(z') = \int_z^h f(z')dz'$ (83)

and for the whole vegetation the total leaf area (Leaf Area Index) LAI (m^2/m^2) is determined:

$LAI = \int_0^h f(z')dz'$. (84)

If the distribution is uniform in a thin canopy, we obtain:

$f(z') = \frac{LAI}{h}$ and $F(z') = LAI\left(1 - \frac{z'}{h}\right)$ (85)

where z' is the height in vegetation considered (m) with respect to the soil surface, z'-axis pointing upwards.

The net solar radiation ϕ (W/m^2) is absorbed as it penetrates the vegetation. From the direct measurements, the radiation attenuation was determined as a function of leaf density. The most suitable type of attenuation [11] is the exponential attenuation at each canopy level z:

$\phi(z') = \phi_0 . exp\,[-0.65F(z') + 0.05\,F(z)^2]$ (86)

At the ground surface, the flux density can be evaluated:

$\phi(0) = \phi_0 . exp\,[-0.65LAI + 0.05(LAI)^2]$ (87)

At the canopy surface, the incident flux density is:

$\phi(h_0) = \phi_0$ (88)

- Initial conditions

$T(z, 0) = T_0$ (89)

2.1.2.4 Numerical resolution

To discretize the heat equation, the implicit finite difference method is used.

It has the following advantages: simplicity of implementation; efficiency; possibility of constructing high order approximations; simple local analysis of accuracy and convergence; low computational cost.

The finite difference method consists in approximating the derivatives of the partial differential equations by means of Taylor developments.

To obtain the mesh, we discretize space and time.

$(z_j, t_n) = ((j-1)\Delta z, (n-1)\Delta t)$ for n = $1, n_{tmax}$ and $j = 1, N$ (90)

where: Δz is the space step and Δt is the time step; n_{tmax} and N are the number of nodes in time and space mesh respectively.

The time derivative of T_{soil} is approximated using the explicit Euler scheme (progressive in time, or "forward").

$$\frac{\partial T_{soil}}{\partial t}(z_j, t_n) \approx \frac{T_{soil,j}^{n+1} - T_{soil,j}^{n}}{\Delta t} \quad (91)$$

The second derivative of T_{soil} with respect to z is approximated using the "centered" scheme.

$$\left(\frac{\partial^2 T_{soil}}{\partial z^2}\right)_j^{n+1} \approx \frac{T_{soil,j+1}^{n+1} - 2T_{soil,j}^{n+1} + T_{soil,j-1}^{n+1}}{\Delta z^2} \quad (92)$$

Substituting relations (27) and (28) into equation (19):

we obtain: $\rho_{sol} c_{p,soil} \frac{T_{soil,j}^{n+1} - T_{soil,j}^{n}}{\Delta t} = \frac{1}{(\Delta z)^2}[\lambda_{soil,j+\frac{1}{2}} T_{soil,j+1}^{n+1} - \left(\lambda_{soil,j+\frac{1}{2}} + \lambda_{soil,j-\frac{1}{2}}\right) T_{soil,j}^{n+1} + \lambda_{soil,j-\frac{1}{2}} T_{soil,j+1}^{n+1}$ (93)

where :

$$\varepsilon = \frac{\Delta t}{\rho_{sol} c_{p,soil}} \frac{1}{\Delta z^2} \quad (94)$$

$$\lambda_{soil,j+\frac{1}{2}} = \frac{1}{2}(\lambda_{soil,j+1} + \lambda_{soil,j}) \quad (95)$$

$$\lambda_{soil,j-\frac{1}{2}} = \frac{1}{2}(\lambda_{soil,j} + \lambda_{soil,j-1}) \quad (96)$$

or :

$$[1 + \varepsilon(\lambda_{soil,j+1} + 2\lambda_{soil,j} + \lambda_{soil,j-1})]T_{soil,j-1}^{n+1} + \varepsilon(\lambda_{soil,j+1} + 2\lambda_{soil,j} + \lambda_{sol,j-1})T_{sol,j}^{n+1} - \varepsilon(\lambda_{soil,j} + \lambda_{soil,j-1})T_{soil,j-1}^{n+1} = T_{soil,j}^{n} \quad (97)$$

The final discretized heat transfer equation is as follows:

$$a_j T_{soil,j-1}^{n+1} + b_j T_{soil,j}^{n+1} + c_j T_{soil,j+1}^{n+1} = d_j \quad (98)$$

with :

$$a_j = -\varepsilon(\lambda_{soil,j} + \lambda_{soil,j-1}) \quad (99)$$

$$b_j = 1 + \varepsilon(\lambda_{soil,j+1} + 2\lambda_{soil,j} + \lambda_{soil,j-1}) \quad (100)$$

$$c_j = -\varepsilon(\lambda_{soil,j+1} + \lambda_{soil,j}) \quad (101)$$

$$d_j = T_{soil,j}^{n} \quad (102)$$

Boundary conditions:

The boundary conditions are discretized using:

- the 'forward' formulation for the boundary condition at the ground surface.

$$\left(\frac{\partial T_{soil}}{\partial z}\right)_j^{n+1} \approx \frac{-3T_{soil,j}^{n+1} + 4T_{soil,j+1}^{n+1} - T_{soil,j+2}^{n+1}}{2\Delta z} \quad (103)$$

-the "backward" formulation for the boundary condition at depth z=e.

$$\left(\frac{\partial T_{soil}}{\partial z}\right)_j^{n+1} \approx \frac{3T_{soil,j}^{n+1} - 4T_{soil,j-1}^{n+1} + T_{soil,j-2}^{n+1}}{2\Delta z} \quad (104)$$

We obtain:

$$T_{soil,N}^{n+1} = \frac{1}{3}(4T_{soil,N-1}^{n+1} - T_{soil,N-2}^{n+1}) ; \quad (105)$$

$$T_{soil,1}^{n+1} = \frac{1}{K_0}[\alpha_0 \Phi_0 + \frac{\lambda}{2\Delta z}(4T_{soil,2}^{n+1} - T_{soil,3}^{n+1}) + h_v T_a^{n+1} + K_1] \quad (106)$$

Initial conditions:

$$T_j^{n+1} = T_0 \quad (107)$$

The resulting tri-diagonal scheme (98), is solved by the Thomas Algorithm combined with the iterative Gauss-Seidel method.

2.2 Validation of the soil thermal model

In order to validate the analytical model, a study was carried out on the modeling of soil temperature, under the meteorological conditions of the city of Adrar in Algeria [11]. The analytical results of soil temperature obtained are compared with the numerical results of Benhammou et al [11] (figure 1). The calculation has been performed over a real time of 12 months. The comparative analysis is done for different depths. The comparison of the temperature profiles for z=0.0; 0.5d; 1.0d; 1.5d; 2.0d and 2.5d on figure 1, shows that there

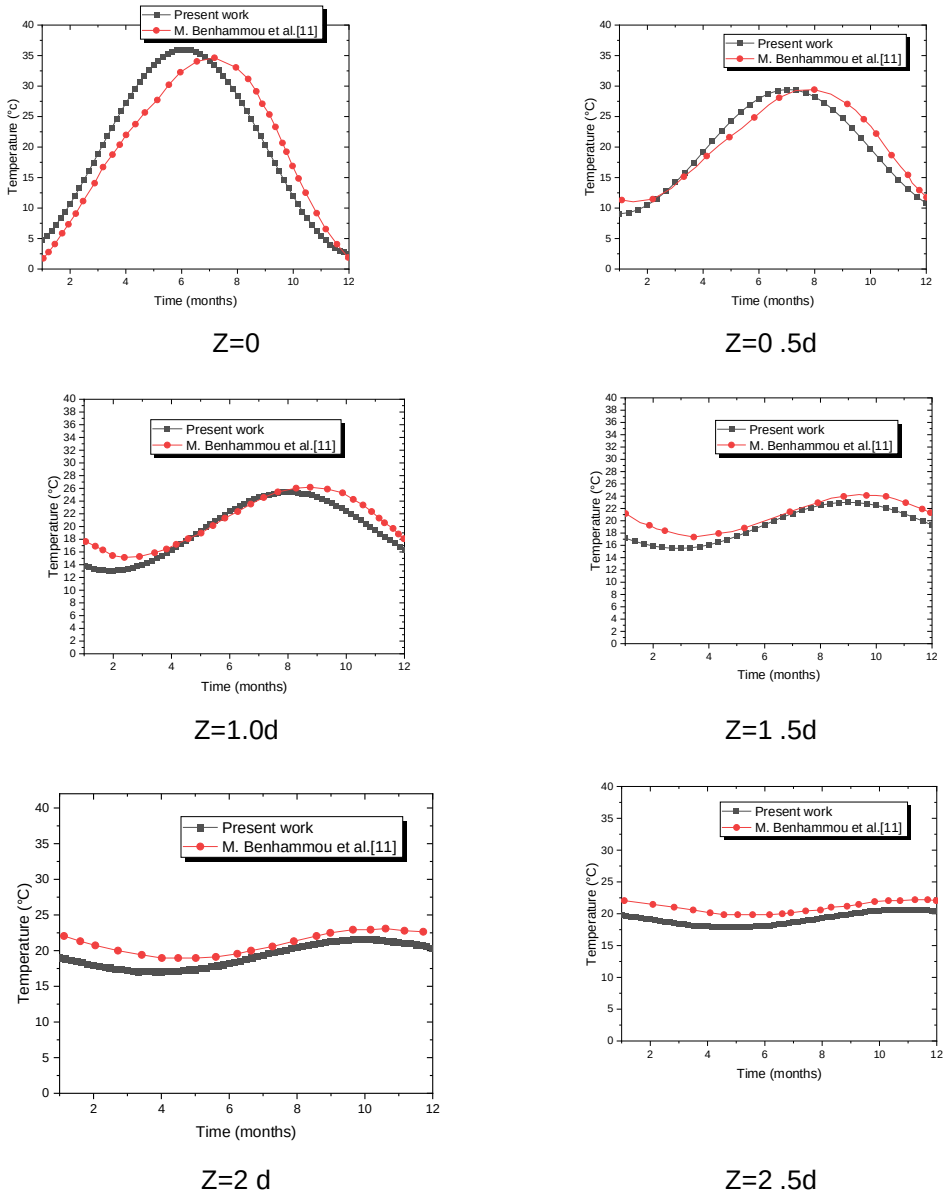

Fig. 1 Variation in soil temperature throughout the year for different depths

is a satisfactory qualitative agreement between the results obtained in the present work and those of Benhammou et al [11]. The discrepancy found at the temperature level can be explained by the difference in the meteorological data used for simulation. We did not find any weather data used by Benhammou et al [11].

3. RESULTS AND DISCUSSION

The simulation is performed using climate data of Togo (Table 2) from 2021.
In this study, three types of dry soils is considered: clay soil, Sandy-clay silt soil and sandy soil whose thermal diffusivities are derived from the experimental study of the nature of the soils and physical properties of M. Benhammou et al. [11] presented in Table 3.

Table 2 Climate data of Togo (National meteological Service of National Aviation Security Agency (*ASECNA*))

Months	Temperature (°C)	Solar Flux Density $(W.m^{-2})$
January	28.5	591.9
February	29.7	714.3
March	29.9	750.0
April	28.7	800.4
May	27.8	705.0
June	26.5	570.8
July	25.4	691.2
August	24.5	584.8
September	25.3	758.6
October	27.1	776.5
November	28.0	690.5
December	28.3	617.0

Table 3 Thermal properties of dry soil [11]

Type of soil	ρ_{soil}(kg/m^3)	α_{soil} (m^2/s)	C_{psoil} (J/kg.°C)
Clay soil	1500	9,69.10-7	880
Sandy-clay silt soil	1800	6,22.10-7	1340
Sandy soil	1780	3,76.10-7	1390

3.1 Heat transfer model in a semi-infinite soil without vegetation cover

In this section, it is presented the analytical solution of heat and mass transfer equation in the case the soil is uncovered of vegetation. The analytical solution allows to determine the depth in the soil at which the thermal wave is attenuated to a given accuracy. Considering daily variations corresponding to a period T=24 hours, the results for different kind of soil: clay soil, sandy-clay silt soil, sandy soil are presented in table 4.

Table 4 Thermal wave attenuation depth

	ϵ_0	Clay soil	Sandy-clay silt soil	Dry sandy soil	Wet sandy soil
z_P (m)	10 %	0,3758889095	0,3011568986	0,2341485896	0,2193585636
	1 %	0,7517778189	0,6023137971	0,4682971791	0,438717127
	0.1 %	1,127666728	0,9034706957	0,7024457687	0,658075690

The results show that for a thermal wave attenuation of 1%, the depth of wave attenuation is about 75 cm for a clay soil compared to 60 cm and 46 cm respectively for a clay-sand silt soil and a purely sandy soil. This depth reaches 01 m when an accuracy of 1/1000 is sought. The results show a reduction in the amplitude of the thermal wave in the soil of 10% at depths of 46 cm for dry sand, 60 cm for sandy-clay silt soil and 75 cm for clay. This means

that a clay soil has a high sensitivity to climatic variations compared to a sandy soil. Thus, the study of the nature of the soil is very essential for the determination of the soil temperature. In the case of a moist sandy soil, a decrease in depth attenuation from 46 cm to 43 cm is observed corresponding to a difference of 0.3 cm. This observation highlights the influence of humidity on the spatial and temporal distribution of the thermal wave in the subsoil. The difference between moist soil and dry soil is the amount of water in the soil. Water is the element in soil that conducts heat, and the soil itself, depending on it's mineral content, is largely an insulator, not allowing heat to pass. Therefore, the water is the transfer agent for thermal conductivity and the more water present in the soil, the more heat is conducted. Moist soil conducts heat while dry soil does not. This explains what the wetter the soil is, the better it conducts.

Figure 2 presents the profile of the attenuation deph of thermal wave versus the attenuation accuracy of the thermal wave in the soil taking into account the effects of the nature of the soil. It shows the depth at which the amplitude of the thermal wave, for different types of soils, is damped. It can be observed that, for each kind of soil, the attenuation deph decreases when the attenuation accuracy of the thermal wave increases. That means that the temperature amplitude is even more damped as the depth of the soil is great. This damping is more sensitive at low depths for sand than for sandy clay silt soil and clay. Then more pronounced for sandy clay silt soil than for clay. These results corroborate very well with the observations made on Table 4.

The variation of soil temperatures with depth is shown in Figure 3. The results show that soil temperatures decrease with depth and stabilize around an average value of 30°C for depths greater than about 5 m. This result confirms the observation made earlier. From this analysis, it can be seen that the sand provides the thermal performance to reach the stable soil temperature at a low depth.

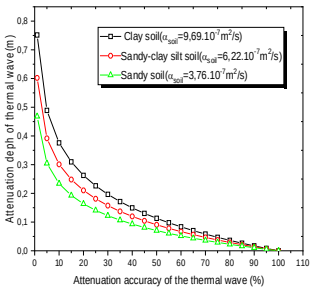

Fig. 2. Attenuation depth versus attenuation accuracy of amplitude of the thermal wave

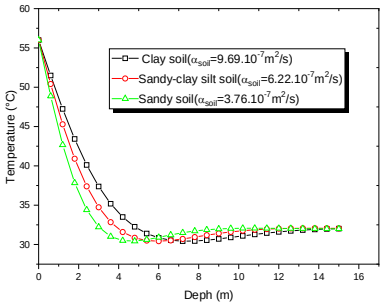

Fig. 3. Temperature variation with depth z for t=24 hours

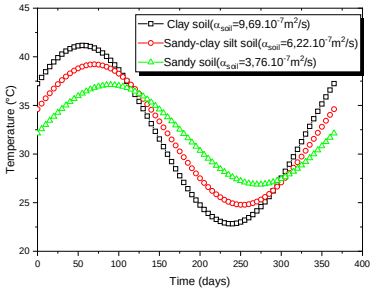

Fig. 4. Variation of soil temperature throughout the year for different thermal diffusivities for z=3 m

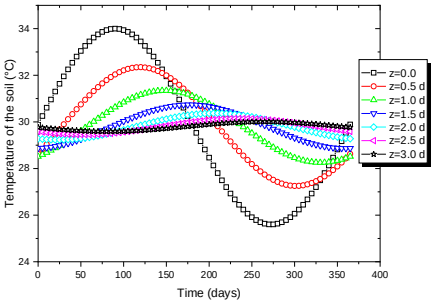

Fig. 5 Variation of soil temperature throughout the year for different depths

Figure 4 shows the variation of soil temperature throughout the year for different soil types. A sinusoidal variation is observed for all diffusivities tested. It can also be seen that as the soil diffusivity increases for different soil types the amplitude of the soil temperature increases.
Figure 5 shows, for different depths, the variation of the soil temperature in correlation with the days in the year. The analysis of this figure shows that the soil temperature follows a sinusoidal variation of time. It can be seen that the amplitude of the temperature signal decreases with increasing depth and beyond a depth of 5 m, the soil temperature no longer has the shape of a sinusoid and stabilizes at around 30°C. It can be observed also in this figure that the vertices of the sinusoids are offset from each other. These observations can be explained by the form of the analytical solution obtained. Indeed, an analysis of the expression of the analytical solution (73) of heat transfer equation in the soil (9) reveals two effects of the depth on the temperature: a damping of the amplitude of soil temperature and a phase shift of temperature as a function of depth.
The results obtained in figure 6 show the evolution of the temperature in the soil for the twelve months of the year. A gradual decrease in temperature can be seen from March to August in the year. The temperature stabilizes at around 28°C at a depth of 5 m. On the other hand, the phenomenon is reversed for the months of September to February, when the soil temperatures increase with depth and stabilize at a depth of 5 m. These results show that during hot periods, the outside air temperature is higher than the soil temperature. In opposite, when it is at cold periods, the soil temperature is higher than ambient temperature. Thus, the soil thermal inertia can be exploited in geothermal systems for cooling or heating buildings in relation to the weather. For the bioreactors facilities, the results shows that the production of biogas, the temperature and moisture distribution in landfills can be affected strongly by the variation of the atmosphere temperature at the top of the landfills and soil temperature at the bottom of the landfills in contact with the soil.

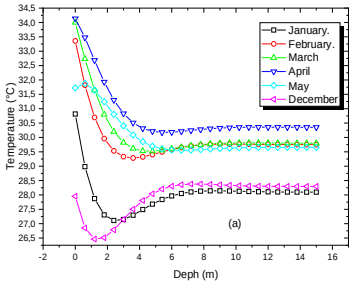

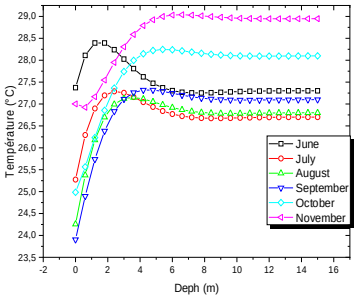

(a) (b)

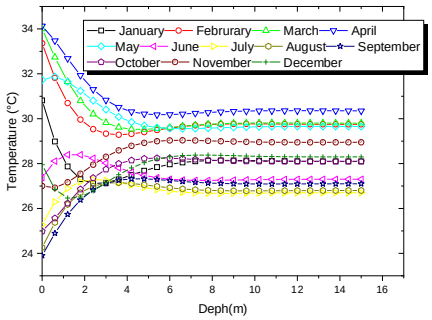

(c)

Fig. 6 Variation of temperature with depth for different months in the year

3.2 Heat transfer model in a semi-infinite soil covered with vegetation

The spatio-temporal distribution model of temperatures in a finite thickness of ground with vegetation cover was simulated by considering a finite thickness layer e=5 m. Indeed, previous analyses showed that for the three types of soil studied, the penetration depth of the thermal wave did not exceed this length. The resolution is done by an iterative numerical method developed in a Fortran environment.

Figure 7 shows the variations of the thermal wave as a function of time at different depths of sandy soil for the months of March and August corresponding respectively to the months during year 2021 when solar radiation is greater and less important in Lome (Togo). Between 6 a.m (t=6 hours). and 6 p.m (t=18 hours) the temperature shows a bell-shaped pattern. The ground temperature rises from 7 a.m (7 hours) to 12 a.m (t=12 hours). It reaches its maximum value around 12 a.m. and starts to decrease until 6 p.m (t=18 hours). From 6 p.m (t=18 hours) to 6 a.m of the following day (t=30 hours). it continues to decrease, but this time more slowly. The evolution of the ground temperature during the day follows that of the solar flux, which is a function of the position of the sun. It can be observed that for the two months the amplitude of the thermal wave reaches its maximum around 12 a.m. During the day, the amplitude of soil temperature decreases when the deph increases. The opposite phenomenon is observed during the night. The temperature is higher when the deph increases due to thermal inertia of the soil. The soil warms up slowly during the day and cools down slowly at night. Indeed, soil has a low thermal conductivity and it is only the surface layer that is heated. The surface of the soil heats up and cools down quickly, while the temperature changes more slowly in the deph of soil.

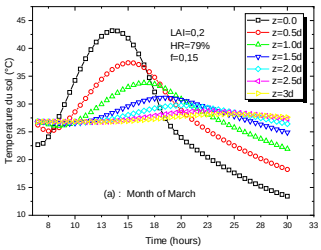

(a)

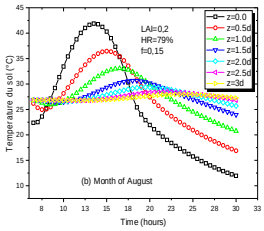

(b)

Fig. 7. Variation in soil temperature during a day in March and August fordifferent depths

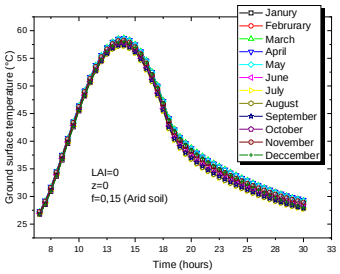

Fig. 8. Evolution of surface temperature according to the months of the year

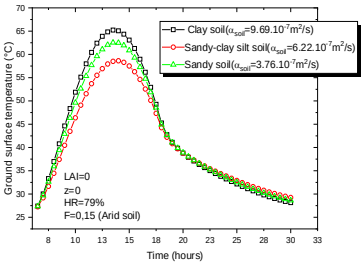

Fig. 9. Evolution of surface temperature according to soil types throughout the year

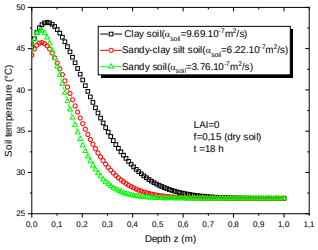

Fig. 10. Temperature variation in the ground

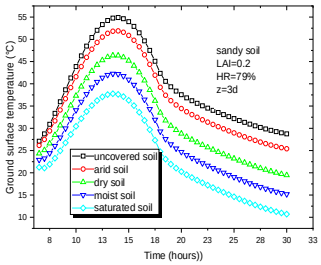

Fig. 11. Evolution of the temperature in the soil as a function of its water saturation state

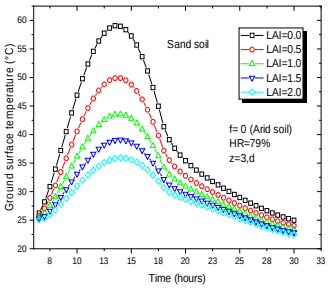

Fig. 12. Influence of vegetation cover on the temporal evolution of soil temperatures

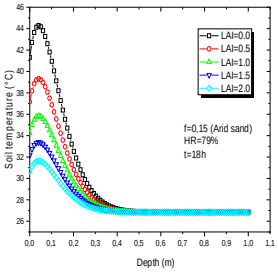

Fig. 13. Influence of vegetation cover on soil temperature variations

Figure 8 presents the evolution of soil surface temperature during a day for the 12 months of the year. The soil considered is arid sandy soil. From January to December, soil surface temperatures vary slightly during the day because of the low ambient temperature difference.

The analysis of figure 9 shows that the properties of the soil influence on the evolution of ground surface temperature. The amplitude of the temperature decreases with the thermal diffusivity. The sandy soil surface temperature is lower than the clay soil surface temperature and higher than the clay-sandy silt soil surface temperature. The difference between the surface temperature of clay soil and the sandy soil surface temperature is small. It is around 2.5°C. This can be explained by the fact that the different arid soils have almost identical thermal diffusivities. On the other hand, there are very significant variations between clay-sandy silt and sandy soil surfaces temperatures because the difference between their thermal diffusivity is significant. The resulting difference in their surface temperature is approximately 7.5°C.

Figure 10 shows the temperature variations as a function of depth in the different types of soil under Lome (Togo) climatic conditions at t=6 p.m (18 hours) for a day of March month which is the hottest month in a year in Togo. It can be observed that the amplitude of the daily thermal wave of the soil gradually decreases in the ground and stabilizes at constant values of 27°C at a depth of 50 to 70 cm depending on the nature of the soil.

Figure 11 illustrates the effects of evaporation phenomena on the temperature distributions in the case of sandy soil. It is considered respectively uncovered, arid, dry, moist and saturated sandy soil. This figure shows a significant influence of the evaporation on the evolution of temperature in the soil. The saturated soil presents a lower temperature and the uncovered soil, the higher temperature. An increase in moisture content decreases the soil temperature. Naturally, moist soil stores more heat resulting in less rising in it temperature.

Figures 12 and 13 illustrate the influence of vegetation cover on ground temperature variations. A decrease in the amplitude of the thermal wave near the surface of the ground, is observed when the Leaf Area Index (LAI) increases. However, its influence on the stabilization depth is not very significant as shown in Figure 13. Stabilization of soil temperatures is observed at a depth of about 40 cm for all LAI with a value of 37°C.

4. CONCLUSION

In this work, it was proposed to study the propagation of thermal waves in the ground under the climatic conditions of Lome (Togo). Indeed, depending on the weather conditions, time in a daily, monthly and yearly period, the outdoor air is subjected to strong variations in

temperature and humidity. Furthermore the ground temperature at a certain deph, varies slightly due to its high thermal inertia.
The proposed heat transfer models predict spatial and temporal variations in ground temperature. The attenuation depth of heat wave in the ground is determined. It is about 5 m and 40 cm, respectively, for yearly and daily simulation with sandy soil. At these dephs, an air/soil exchanger can take advantages of the high inertia and pump frigories from the basement to pre-condition the thermal and hygrometric ventilation air in the rooms. These depths levels are also useful for the installation of underground electronic equipment and more particularly for batteries used to store electrical energy in photovoltaic systems. Knowledge of the thermal behavior of the soil is also important in understanding the biodegradation of waste in bioreactors facilities. The biogas production and the distribution of temperature and moisture in landfills, can be affected significantly by the variation of the temperature at the surface of the landfills cell and by soil temperature variation at the bottom of the landfills cell.
The simulation results obtained showed that the penetration depth of the thermal wave depends not only on the climatic conditions of the site, but also on the nature of the soil, the latent exchanges of water evaporation and the characteristics of the vegetation cover. Neglecting these parameters can significantly affect the accuracy of the thermal wave model of the soil for a given site.

REFERENCES

1. Rankinen K, Karvonen T, Butterfield D. A simple model for predicting soil temperature in snow-covered and seasonally frozen soil: model description and testing. Hydrology and Earth System Sciences. 2004; 8(4):706–716.
https://doi.org/10.5194/hess-8-706-2004

2. Sodha MS, Sharma AK, Singh SP, Bansal NK, Kumar A. Evaluation of an earth-air tunnel system for cooling/heating of a hospital complex. Building and Environment. 1985; 20(2): 115-122.
https://doi.org/10.1016/0360-1323(85)90005-8

3. Mavroyanopoulos GN, Kyritsis S. The performance of a greenhouse heated by an earth - air heat exchanger. Agricultural and Forest Meteorology. 1986; 36(3): 263-268.
https://doi.org/10.1016/0168-1923(86)90040-7

4. Tzaferis A, Liparakis D, Santamouris M, Argiriou A. Analysis of the accuracy and sensitivity of eight models to predict the performance of earth-to-air heat exchangers. Energy and Buildings. 1992; 18(1) : 35-43.
https://doi.org/10.1016/0378-7788(92)90049-M

5. Mihalakakou G, Santamouris M, Asimakopoulos D, Papanikolaou N. Impact of ground cover on the efficiency of earth-to-air heat exchangers. Applied Energy. 1994; 48(1):19-32.
https://doi.org/10.1016/0306-2619(94)90064-7

6. Dolschak K, Gartner K, Berger TW. A new approach to predict soil temperature under vegetated surfaces. Modeling Earth Systems and Environment. 2015; 1:32
DOI 10.1007/s40808-015-0041-2

7. Islam, MA, Lubbad R, Ghoreishian Amiri SA, Isaev V, Shevchuk Y, Uvarova AV, Afzal MS

Kumar A. Modelling the seasonal variations of soil temperatures in the Arctic coasts. Polar Science. 2021; 30, 100732.
https://doi.org/10.1016/j.polar.2021.100732

8. Liu H, Wang X, Wang, Y Zhu, K. Numerical analysis of ground temperature response characteristics of a space-heating ground source heat pump system by utilizing super-long flexible heat pipes for heat extraction. Energy and Buildings. 2021; 244, 110991.
https://doi.org/10.1016/j.enbuild.2021.110991

9. Mahdi MH, Abduljabbar HM. An analytical study of soil temperature with respect to its salinity. Technologies and Materials for Renewable Energy, Environment and Sustainability. 2019; 2190. 0, 020009-1–020009-8;
https://doi.org/10.1063/1.5138495

10.Guojie H, Zhao L, Wu X, Li R, Wu T et al. An analytical model for estimating soil temperature profiles on the Qinghai-Tibet Plateau of China. Journal of Arid Land. 2016; 8(2): 232–240.
DOI:10.1007/s40333-015-0058-4

11. Benhammou M, Draoui B. Modélisation de la température en profondeur du sol pour la région d'Adrar - Effet de la nature du sol. Revue des Energies Renouvelables. 2011 ; 14 : 219 – 228. French

12. Sodha MS, Bansal NK, Seth AK. Variance of the ground temperature distribution. Applied Energy. 1981; 8(4): 245-54.
https://doi.org/10.1016/0306-2619(81)90021-0

13. Ozgener O, Ozgener L, Tester JW. A practical approach to predict soil temperature variations for geothermal (ground) heat exchangers applications. International Journal of Heat and Mass Transfer. 2013; 62: 473-80.
https://doi.org/10.1016/j.ijheatmasstransfer.2013.03.031

14. Bowen A, Clark E, Labs K. Passive and Hybrid Cooling Conference. Eds., Proc Int. 1981.

15. Zhan M, Xia L, Zhan L, Wang Y. Evaluation and Analysis of Soil Temperature Data over Poyang Lake Basin, China. Advances in Meteorology. 2020; ID 8839111.
https://doi.org/10.1155/2020/8839111

16. Singh RK, Sharma, R.V. Numerical analysis for ground temperature variation. Geotherm Energy. 2017; 5(22).
https://doi.org/10.1186/s40517-017-0082-z